



UNIVERSITY OF LEEDS

This is a repository copy of *Scale-up of an RF heated micro trickle bed reactor to a kg/day production scale*.

White Rose Research Online URL for this paper:
<http://eprints.whiterose.ac.uk/124504/>

Version: Accepted Version

Article:

Fernández, J, Chatterjee, S, Degirmenci, V et al. (1 more author) (2015) Scale-up of an RF heated micro trickle bed reactor to a kg/day production scale. *Green Processing and Synthesis*, 4 (5). pp. 343-353. ISSN 2191-9542

<https://doi.org/10.1515/gps-2015-0035>

© 2015, De Gruyter. This is an author produced version of a paper published in *Green processing and synthesis*. Uploaded in accordance with the publisher's self-archiving policy.

Reuse

Unless indicated otherwise, fulltext items are protected by copyright with all rights reserved. The copyright exception in section 29 of the Copyright, Designs and Patents Act 1988 allows the making of a single copy solely for the purpose of non-commercial research or private study within the limits of fair dealing. The publisher or other rights-holder may allow further reproduction and re-use of this version - refer to the White Rose Research Online record for this item. Where records identify the publisher as the copyright holder, users can verify any specific terms of use on the publisher's website.

Takedown

If you consider content in White Rose Research Online to be in breach of UK law, please notify us by emailing eprints@whiterose.ac.uk including the URL of the record and the reason for the withdrawal request.



eprints@whiterose.ac.uk
<https://eprints.whiterose.ac.uk/>

Scale-up of strategies of a multi catalyst zone radio frequency heated micro trickle bed reactor

Javier Fernández ^a, Sourav Chatterjee ^b, Volkan Degirmenci ^{a, b}, Evgeny V. Rebrov ^{a, *}

^a School of Engineering, University of Warwick, Coventry CV4 7AL, UK

^b School of Chemistry and Chemical Engineering, Queen's University Belfast, Belfast BT9 5AG, UK

* E-mail: E.Rebrov@warwick.ac.uk

Abstract

The scale up of an isothermal micro-trickle bed reactor operated under radio frequency (RF) heating has been performed. The effect of the reactor length, tube diameter and number of parallel tubes on the temperature non-uniformity parameter has been studied. The axial and radial temperature profiles were calculated using a 2D convection and conduction heat transfer problem with heat transfer properties determined in Ref. A periodic repetition of heating and catalytic zones in the axial direction allows to keep the axial temperature gradient within 2 K. A radial temperature gradient of 2 K starts to develop above a diameter of 28.5 mm.

Keywords: Scale-up; micro reactor; trickle bed, fine chemicals, radio frequency, magnetic nanoparticles.

1. Introduction

The fine chemicals synthesis processes require the production of valuable compounds with a high degree of purity [1]. These processes, often multiphase in nature, commonly follow stoichiometric organic routes which generate substantial amounts of by products and tend to suffer from low product yields [2]. Stringent environmental regulations based on good manufacturing process make it necessary to replace existing stoichiometric processes with catalytic ones [3]. Among them, hydrogenation is an important type of catalytic gas-liquid-solid reactions in pharmaceutical and fine chemical industries [3].

Batch processes are often chosen because reaction optimised conditions can directly be transferred from a laboratory scale to a production scale. However the stirred tank reactors have various drawbacks, such as labour intensive operation and poor performance as a result of insufficient mixing. In this way, development of new and innovative reactor systems for catalytic chemical reactions has gained considerable attention recently [4, 5]. In particular structured reactors are considered to offer numerous advantages in processing of moderate amounts of liquid reactants when compared with traditional stirred tank reactors. Improved mass and heat transfer properties enable the use of more intensive reaction conditions that result in higher reaction rates than those obtained with conventional reactors. Furthermore heat management during exothermic reactions can properly be tuned.

Trickle bed reactors could be superior to stirred tank reactors, as there is no need for catalyst filtration [6]. Trickle bed reactors are employed in petrochemical and biochemical industry as well as in waste treatment applications [7]. However, poor heat transfer behaviour of conventional trickle bed reactors and liquid flow maldistribution [8] often result in lower selectivities and catalyst deactivation. [9]. The former is often caused by the fact that the heat is supplied from an external heating source and the net energy

flux transferred to the reactor is a strong function of the wall heat transfer coefficient and thermal conductivity of bed [10]. Several studies discuss the effect of these parameters on reactor performance [11, 12]. High thermal inertia of furnaces and low thermal conductivity of reactor bed, make it difficult to maintain isothermal conditions. The heat transfer to the centre of a catalyst layer can still be a limiting step. Alternative means of energy supply that would facilitate rapid and uniform volumetric heating, are therefore of interest.

Zonal radiofrequency heating (RF) of the structured support can enhance energy utilisation. This is a scalable method proven at both laboratory and industrial conditions. In such reactor, the reactor bed is packed with alternating zones of catalyst and magnetic particles or the catalyst is deposited onto magnetic core as a thin shell. By the rational design of the bed packing, a near isothermal conditions can be created inside the catalyst bed [5]. Moreover, combining continuous operation and RF heating as an alternative energy source, allows the accurate control of residence times in chemical processes. The synergism of RF heating and continuous operation leads to a process intensified approach which improves the selectivity and product yield thus increasing the output per unit volume of plant space [13, 14].

The scaling up of an RF heated reactor is to some extent similar to a microwave heated flow reactor. Most of studies in this area evaluate the limitations related to the volumetric scale-up while using standard microwave equipment available in the market [15]. Organ et al. in their work on microwave assisted organic synthesis have discussed the possibility of parallelization of reactor tubes [16]. While this work does not focus on scale-up, it addresses the possibility of synthesis of an organic library in multiple parallel tubes.

One of the suitable approaches for scaling up in continuous synthesis under RF heating is numbering up. The numbering-up approach is based, on one hand, on numbering up of

heating and catalytic zones in the axial direction inside a single tube [17] and, on the other hand, on parallelization of tubular structured reactors with a channel diameter in the millimeter range [18] which can still be positioned inside a single RF coil. The former methodology has been employed in our previous study, where several heating and catalytic zones were placed inside a 70 mm long single tube reactor. Until recently, the later methodology presented itself as a challenge as it requires an equal gas and liquid flow distribution among all parallel tubes. To solve this problem, Al-Rawashdeh et al. developed a novel concept for a barrier based multiphase flow distributor [19]. This distributor allows to obtain a uniform distribution of the gas and liquid flows over the microchannels when the pressure drop over the upstream barrier channels is about 5-20 times higher than the pressure drop over the corresponding reactor channels. Gas-liquid channelling is prevented at equal pressures in the gas and liquid manifolds. The concept has been proven in a wide range of liquid flow rates and liquid to gas ratios [20]. With such approach, a multitubular design of RF heated micro-trickle bed reactor becomes feasible.

There exists also a possibility to increase the tube diameter upon scale up. This is an additional advantage of RF heating as compared to microwave heating as the penetration depth of RF waves is in the meter range. Therefore, the magnetic field remains rather uniform over the reactor cross section and it depends mainly on the coil geometry rather than on magnetic properties of the absorbing material and therefore temperature independent. However, this scale up approach still should be based on the modelling as the heat transfer behaviour as characteristic time for conduction changes as the reactor diameter increases.

This work reports the scale up of a RF heated micro trickle bed reactor by using a multitubular approach. This is achieved, among others, by providing a uniform

temperature distribution in all parallel tubes of the reactor assembly. The performance of the multitubular assembly in hydrogenation of 2-methyl-3-butyne-2-ol was evaluated and compared with a single tube reactor. The temperature profiles were obtained by a 2D convection and conduction model with a heat generation term accounting for the actual distribution of magnetic field inside the catalyst bed. The obtained temperature profiles were validated experimentally for a selected number of experiments.

2. Modelling

The steady-state temperature profiles in the reactor (length 210 mm, diameter 5 –50 mm) were obtained by a 2D convection and conduction model [5, 17] which was solved numerically in COMSOL Multiphysics 5.0. Around 100,000 mesh elements were used to reach mesh independent solutions in all calculations. Heat transfer phenomena in the RF heated reactor are described by the conservation equations of mass, momentum and energy leading to a set of non-linear partial differential equations. To simplify the analysis, the fluid flow is assumed to be non-compressible and the catalyst particles are assumed to be spherical with a diameter d_p . Moreover, the catalyst bed is treated as a homogeneous porous medium with porosity ε_b and permeability K . Based on the above assumptions, the governing equations for the mass conservation and fluid flow can be written as,

$$\nabla \cdot (\varepsilon_b \rho \vec{V}) = 0 \quad (1)$$

$$\frac{1}{\varepsilon_b^2} \nabla \cdot (\rho \vec{V} \vec{V}) = \nabla \cdot \left[-p \vec{I} + \frac{\mu}{\varepsilon_b} (\nabla \vec{V} + (\nabla \vec{V})^T) - \frac{2\mu}{3} \vec{I} \nabla \cdot \vec{V} \right] + S_u \quad (2)$$

where \vec{V} is the superficial velocity, μ is the viscosity, p is pressure. The source term, S_u , term:

$$S_u = -\frac{\mu}{K}\vec{V} + \frac{\rho C_F}{\sqrt{K}} |\vec{V}|\vec{V} \quad (3)$$

K is the permeability and C_F is the Forchheimer drag coefficient for a packed bed of spherical particles with homogenous porosity can be respectively given as,

$$K = \frac{d_p^2 \varepsilon_b^3}{150(1-\varepsilon_b)^2} \quad (4)$$

$$C_F = \frac{1.75}{\sqrt{150\varepsilon_b^{1.5}}} \quad (5)$$

The heat transfer in porous media is described by equation 6;

$$\nabla \cdot (\varepsilon_b \rho C_p \vec{V} T) = \nabla \cdot (\lambda_{eff} \nabla T) + q_V''' + h_w a (T - T_\infty) \quad (6)$$

where, a is the external wall area per unit of the reactor volume, λ_{eff} is the effective thermal conductivity of the catalyst bed, h_w is the wall heat transfer coefficient, T is the temperature, ρ is the fluid density, q_V''' is the volumetric heat generation and C_p is the fluid specific heat capacity. q_V''' is proportional to the magnetic field which is adapted from Mispelter et al. [21];

$$q_V''' = q_0 \left[\frac{z+l/2-L/2}{\sqrt{r^2+(z+l/2-L/2)^2}} - \frac{z-l/2-L/2}{\sqrt{r^2+(z-l/2-L/2)^2}} \right] \quad (7)$$

where, q_0 is the maximum volumetric heat generation at the centre of the coil, l is the length of the coil and L is the length of the reactor. q_V''' is zero in the catalytic zones.

The no-slip boundary condition was used at the reactor walls. The actual inlet liquid velocity and an outlet pressure of 1 bar were chosen as boundary conditions for the fluid flow model. For the heat transfer case, heat flux at the reactor walls and an inlet

temperature of 20 °C were chosen as boundary conditions. The fluid properties of methanol were used in simulations.

The catalyst bed was segmented into several sections positioned between adjacent heating zones. The kinetic model for hydrogenation of 2-methyl-3-butyn-2-ol was adopted from [22] to calculate the conversion. The kinetic parameters are listed in Table 1 and the reaction mechanism is given in scheme 1. Simulations were performed to determine the minimum number and the length of each heating zone which would provide an isothermal profile in the fixed bed. The reactor parameters were adapted from [5] and they are listed in Table 2. A higher volumetric heat generation rate of 0.3 W/cm³ was fixed in the preheating section to reduce its length. In an actual reactor, this is done by providing a higher ferrite loading in the preheating zone.

Insert scheme 1 here.

Insert Tables 1 and 2 here.

3. Experimental

A vertically positioned tubular quartz reactor (I.D. 10 mm, O.D. 12.7 mm) was filled with several zones of nickel ferrite particles [23] (106-150 μm) separated by catalytic zones and placed inside an induction coil (I.D. 26 mm, length 210 mm) connected to an RF generator operating at 180 kHz (Easyheat Ambrell). The structured bed was fixed from both sides with two porous PEEK plates. The reactor and the coil were insulated with glass wool of 4 cm thickness.

Insert Figure 1 here

A fibre optic temperature sensor (FISO Scientific) was placed inside a glass capillary (O.D. 3.0 mm accuracy of 0.1 °C) along the central axis of the bed for temperature measurements. The temperature at a specific position was controlled with the LABVIEW software. The reaction samples containing reactants and the product were collected for GC analysis. The samples were analysed by an offline GC (Varian 430, column: CP-Sil 5 CB) equipped with an FID detector.

4. Results and discussion

4.1 Scale-up in the axial dimension

It has been noticed [17] that in order to keep a low temperature non-uniformity, it is necessary to split a single catalytic zone into several sections separated by heating zones. One catalytic and one heating zone form a single periodic unit which, in principle, can be repeated in the axial direction if the RF field uniformity remains the same. That assumption would be valid if (i) the heat released by an exothermic hydrogenation reaction is at least an order of magnitude below then that produced by the magnetic particles in heating zones and (ii) the heat loss by natural convection via the external wall remains the same over the entire length of the reactor. In that case the net heat generation rate over a single periodic unit is equal to the rate of heat loss to the environment, the latter being determined by natural convection.

The first assumption can be satisfied at a relatively high concentration of magnetic particles in the heating zones. In this case, any change of reaction rate would not influence the overall heat production rate. The second assumption is valid for a relatively short reactor ($L/d < 100$) when the development of natural convection boundary layer occurs in the laminar regime.

The temperature profile in the single tube reactor was obtained by solution of a 2D convection and conduction model (Eqs. 1-5). In this design, ten catalyst bed sections with a length of 10 mm were separated by eleven heating zones with a length of 5 mm. The first heating zone was required to preheat the reaction mixture from room temperature to the reaction temperature.

Insert Figure 2 here

It can be seen that the temperature rises from 17 °C to the reactor set-point (41 °C) within the first 35 mm of the reactor length and then remains rather constant (Figure 2a). Local temperature maxima develop within the heating zones while local minima are observed in the catalytic zones. The periodic repetition of one catalytic and one heating zone allows to keep the temperature non uniformity within 2 K. The MBY conversion increases linearly with the residence time in the catalytic zones following a zero order kinetics until a conversion of 99% is reached in catalytic zone 6 (Figure 2b). The subsequent catalytic layers (from zone 7 to 11) can be added in case of catalyst deactivation or when a higher liquid flow rate would be required. Otherwise they can be omitted and replaced by inert material. As the total pressure drop does not exceed 1 kPa, it is rather straightforward to build up a reactor bed of any length by repeating the single periodic unit.

4.2 Scale-up in the radial dimension

The scale-up in the axial direction can potentially increase the productivity of a single zone reactor by an order of magnitude. Still there is a possibility to extend the catalyst volume in the radial dimension while maintaining near-isothermal operation of the reactor bed. In order to investigate the effect of reactor diameter on the temperature non-

uniformity parameter and conversion, temperature distribution was investigated in reactors with diameter of 5.0, 10, 15, 25 and 50 mm. Those will be designated as R-a, where a is the diameter in mm, hereafter.

As opposed to the axial scale-up, the intensity of the magnetic field changes in the radial direction, therefore the heat generation term cannot be considered as constant over the cross section of the reactor. Therefore, the heat generation term was introduced as a function of radial position. The total amount of heat was adjusted to keep the same average temperature in reactor. This is due to the fact that volumetric heat generation rate increases faster ($\sim r^3$) than the external surface area ($\sim r^2$) as the diameter increases. Therefore the amount of magnetic material in the heating zones was reduced as the reactor diameter increases.

The temperature distribution in the R-5, R-15 and R-50 reactors is shown in Figure 3a. It can be seen that there is no radial temperature gradient in the R-5, a small radial temperature gradient starts to develop in the downstream section of R-15, and a substantial gradient develops in R-50 as the temperature decreases towards the outer surface.

Insert Figures 3, 4 here

The temperature non-uniformity results in different reaction rates over the reactor cross section and this results in different conversion levels in these 3 reactors as shown in Figure 3b. A temperature difference of 2 K between the wall temperature and centre axis temperature is created at a diameter of 15 mm (Figure 4). Therefore this diameter is chosen for the subsequent numbering up study. This reactor can accommodate a 9-fold amount of catalyst which results in a comparable enhancement in productivity as that in the axial scale-up.

4.3 Scale up by numbering up

Increasing the reactor dimensions has a beneficial effect as the production rate increases by two orders of magnitude. Still there exists a possibility to increase the production rate via a numbering up approach. Due to their lower frequency levels, RF waves have a larger penetration depth than microwaves and hence could find better application in larger size reactors. As the penetration depth of RF field is much higher as compared to the tube diameter (15 mm), the intensity of magnetic field remains relatively constant over the cross section of a single tube. This is impossible for most liquids heated by microwaves. However, there is a distribution of magnetic field in the radial dimension of a coil. Upscaling of current RF systems, to provide a uniform magnetic field pattern in commercial-scale processes, still remains a major challenge. This results in different steady state conversions in a central and outer tubes in a multitubular reactor which consists of seven parallel tubes: one central and six outer tubes.

Being in the highest field intensity region, the central tube gave the highest conversion (Figure 5a). The outer tubes being exposed to a weaker magnetic field as compared to the central tube gave lower conversion. This is due to the difference in local temperature distribution both in axial (Figure 5b) and radial directions (Figure 5c and d). The average temperature in the central tube is 366 K while it is 359 K in the outer tubes. This results in a 5% difference in the overall MBY conversion. Such difference can be considered as acceptable for the most of industrial applications. However if a higher degree of product uniformity is required, it is better to keep the central reactor position empty.

Insert Figure 5 here.

5. Experimental validation

The reactor design was verified experimentally in the hydrogenation of 2-methyl-3-butyn-2-ol (MBY). The reactor was loaded with three, four or five catalyst zones containing the 1.2 wt% Pd/TiO₂ catalyst (50 mg per zone) while the remaining catalytic zones were filled with an inert material which has the same thermal properties as the actual catalyst. The initial concentration of MBY was fixed at 0.7 mol/L and the liquid flow rate was fixed at 0.1 mL/min. A rather good agreement between experimental and modelling results was observed. It can be seen that temperature at the axial positions from $x = 35$ to 200 mm remains within 2 K from the reactor set-point of 313 K. (Figure 6a). The MBY conversion and MBE selectivity also demonstrated a good agreement with the model predictions. Figure 5b shows a comparison between experimental and modelling results for a configuration with five catalytic layers. It can be seen that an MBY conversion of 94 % and MBE selectivity of 70 % were obtained in this experiment which is in an excellent agreement with predictions made by the reactor model. A pressure drop of 1 kPa was observed in this reactor configuration which is in line with the theoretical prediction (Figure 2b). The conversion remained stable for several days of operation without substantial increase in the pressure drop. This could justify the feasibility of the chosen scale-up approach. Furthermore, it can be concluded that the 2D convection and conduction model could adequately predict the reactor behaviour.

Insert Figure 6 here.

6. Scale up methodology

The scale-up method is divided in three steps – a repetition of a single periodic unit composed of one catalytic and one heating zone (Figure 7a) along the reactor length

(Figure 7b), an increase of reactor diameter (Figure 7c) and numbering up step (Figure 7d).

Insert Figure 7 here.

The repetition of the single periodic unit results in a scale-up factor of at least 11, which is proven in this study. There is still a possibility to increase the number of periodic units in the axial direction as the pressure drop over the reactor bed remains relatively low and it does not result in densification of the reactor bed.

The scale-up in radial direction depends on the thermophysical properties of the catalytic bed. In general, trickle bed reactors suffer from rather low effective thermal conductivity which does not allow to increase the reactor diameter without substantial increase in the radial temperature gradient. In this study, the titania support was used for the Pd catalyst, which has relatively low thermal conductivity. This still allows to increase the reactor diameter by 3 times as compared to laboratory scale reactor, which results in a 9-fold increase of productivity. A combination of axial and radial scale up could provide a two order of magnitude increase in production rate (Table 3).

Insert Table 3 here.

Finally, scale-up by numbering up allows to accommodate up to 7 parallel tubes inside a typical RF coil. while there is a substantial difference between the central and outer tubes which is due to different intensity of magnetic field at these positions. This non-uniformity can further be adjusted by placing different amounts of ferrite material in the central and outer tubes. A higher loading of magnetic material in the heating zones would compensate for lower intensity of magnetic field in the peripheral tubes.

In total a scale up factor of almost 700 (11 x 9 x 7) can be achieved in this approach. This translates in an overall production rate of 0.5 kg of product per day. This design requires an efficient gas liquid distributor to uniformly feed a system of parallel tubes.

7. Conclusions

A scale-up method was proposed for a micro trickle bed reactor. The method is divided in three steps – a repetition of a single periodic unit composed of one catalytic and one heating zone along the reactor length, an increase of reactor diameter and numbering up step. This scale-up approach is based on maintaining the temperature non uniformity parameter in the reactor at the constant level. It requires only lab scale data and it reduces significantly the risk of failure during the initial scale-up of the process.

The optimum reactor configuration was simulated using a convection and conduction heat transfer model and the numerical results were in a very good agreement with experimental data. The overall productivity in a hydrogenation reaction was increased by a factor of 700 using this approach.

Acknowledgements

The financial support provided by the European Research Council (ERC), project 279867, is gratefully acknowledged.

Nomenclature

B	magnetic field (T)
C_p	heat capacity (J/kg K)
C_F	Forchheimer drag coefficient
E_a	activation energy (kJ/mol)
h_w	wall heat transfer coefficient (W/m ² K)
I	identity matrix
l	length of the induction coil (mm)
L	reactor length (mm)
P	pressure (Pa)
q_V'''	volumetric heat generation (kW/m ³)
r_i	reaction rate of component i (mol/m ³ s)
t	time (s)
T	temperature (K)
u	gas superficial velocity (m/s)
\vec{V}	superficial velocity (m/s)
z	spatial coordinate (m)

Greek letters

ΔH_{ads}	enthalpy variation for adsorption (kJ/mol)
ρ	density (kg/m ³)
ϵ_b	bed porosity (-)
k	thermal conductivity (W/m·K)
μ	viscosity (cP)
K_i	Equilibrium adsorption constant for component i
k_i	Kinetic constant for component i (mol/kg _{cat} s Pa)
λ_{eff}	Effective thermal conductivity
δ	Temperature non-uniformity parameter (%)

Figure captions

- Figure 1. The schematic representation of the reactor showing heating and catalytic zones.
- Figure 2. Simulated a) temperature b) MBY conversion and pressure drop as a function of axial position in the 11 zone micro trickle bed reactor. Liquid flow rate: 0.1ml/min gas flow rate: 3.0 ml/min (STP) volumetric heat generation rate: 410 kW/m³.
- Figure 3. Temperature (a-c) and MBY conversion (d-f) maps in the 11 zone reactors. Reactors: (a, d) R-5 mm, (b, e) R-15, (c, f) R-50 mm. Reaction conditions are the same as those in Figure 2.
- Figure 4. The temperature non-uniformity as a function of reactor radius. Reaction conditions are the same as those in Figure 2.
- Figure 5. (a) MBY conversion and (b) centre axis temperature in the 11 zone R-15 reactors as a function of axial position, (c, d) temperature maps of R-15 reactor positioned (c) in the centre of the coil (d) near the edge (See Figure 7). Reaction conditions are the same as those in Figure 2.
- Figure 6. (a) Measured (symbols) and predicted (line) temperature along the center axis in the 11 zone R-5 reactor. (b) Measured and predicted MBY conversion and MBE selectivity in the 5 catalytic zone R-5 reactor. Reaction conditions are the same as those in Figure 2.
- Figure 7. Schematic representation of the scale-up methodology. (a) laboratory scale micro trickle bed reactor, (b) axial scale-up, (c) radial scale-up, (d) scale up by numbering up.

Table 1. Kinetic parameters for MBY hydrogenation.

Parameter	Unit	Value
k_{10}	s^{-1}	5×10^8
k_{20}	s^{-1}	6×10^7
k_3	s^{-1}	2.4×10^{-4}
E_{MBA}	J/mol	60300
E_{MBE}	J/mol	42000
K_Y	m^3/mol	20
K_E	m^3/mol	3.5×10^{-2}
K_A	m^3/mol	1.3×10^{-2}

Table 2. Thermo physical reactor parameters.

Parameter	Unit	Value
Heat transfer coefficient	$W/(m^2 \cdot K)$	4.5
Effective thermal conductivity of bed	$W/(m \cdot K)$	4.0
Ferrite density	kg/m^3	5000
Ferrite specific heat capacity	$J/(kg \cdot K)$	700
Catalyst density	kg/m^3	2460
Catalyst specific heat capacity	$J/(kg \cdot K)$	770
Bed porosity	-	0.43

Table 3. Scale up factors for different methods

	A	R	N	A+R	A+N	A+R+N
Scale up factor	11	9	7	99	77	693

A= axial, R = radial, N = numbering up

References

- [1] Mohamed HM, TrAC, Trends Anal. Chem. 2015, 66, 176-192.
- [2] Pfaltzgraff LA, Clark JH, In Advances in Biorefineries, Waldron, K (Ed.) Woodhead Publishing: Amsterdam, 2014, p 3-33.
- [3] Mills PL, Chaudhari RV, Catal. Today 1997, 37, 367-404.
- [4] De Wilde J, Froment GF, Fuel 2012, 100, 48-56.
- [5] Chatterjee S, Degirmenci V, Aiouache F, Rebrov EV, Chem. Eng. J. 2014, 243, 225-233.
- [6] Stitt EH, Chem. Eng. J. 2002, 90, 47-60.
- [7] Al-Dahhan MH, Larachi F, Dudukovic MP, Laurent A, Ind. Eng. Chem. Res. 1997, 36, 3292-3314.
- [8] Boelhouwer JG, Piepers HW, Drinkenburg AAH, Chem. Eng. Sci. 2001, 56, 1181-1187.
- [9] Hessel V, Angeli P, Gavriilidis A, Loewe H, Ind. Eng. Chem. Res. 2005, 44, 9750-9769.
- [10] B.V, Sastry KKN, Comput. Chem. Eng. 1999, 23, 327-339.
- [11] Lamine AS, Gerth L, Le Gall H, Wild G, Chem. Eng. Sci. 1996, 51, 3813-3827.
- [12] Houlding TK, Rebrov EV, Green Process. Synth. 2012, 1, 19-31.
- [13] Houlding TK, Tchabanenko K, Rahman MT, Rebrov EV, Org. Biomol. Chem. 2013, 11, 4171-4177.
- [14] Houlding TK, Gao P, Degirmenci V, Tchabanenko K, Rebrov EV, Mater. Sci. Eng. B 2015, 193, 175-180.
- [15] Matsuzawa M, Togashi S, Hasebe S, J. Therm. Sci. Tech. 2011, 6, 69-79.
- [16] Comer E, Organ MG, Chem. Eur. J. 2005, 11, 7223-7227.
- [17] Chatterjee S, Degirmenci V, Rebrov EV, Chem. Eng. J. 2015, In press.
- [18] Patil NG, Benaskar F, Rebrov EV, Meuldijk J, Hulshof LA, Hessel V, Schouten JC, Ind. Eng. Chem. Res. 2012, 51, 14344-14354.
- [19] Al-Rawashdeh M, Fluitsma LJM, Nijhuis TA, Rebrov EV, Hessel V, Schouten JC, Chem. Eng. J. 2012, 181-182, 549-556.
- [20] Al-Rawashdeh M, Yu F, Nijhuis TA, Rebrov EV, Hessel V, Schouten JC, Chem. Eng. J. 2012, 207-208, 645-655.
- [21] Mispelter J, NMP probeheads for biophysical and biomedical experiments, Imperial College Press: London, 2006.
- [22] Rebrov EV, Klinger EA, Berenguer-Murcia A, Sulman EM, Schouten JC, Org. Process Res. Dev. 2009, 13, 991-998.
- [23] Gao P, Hua X, Degirmenci V, Rooney D, Khraisheh M, Pollard R, Bowman RM, Rebrov EV, J. Magn. Magn. Mater. 2013, 348, 44-50.

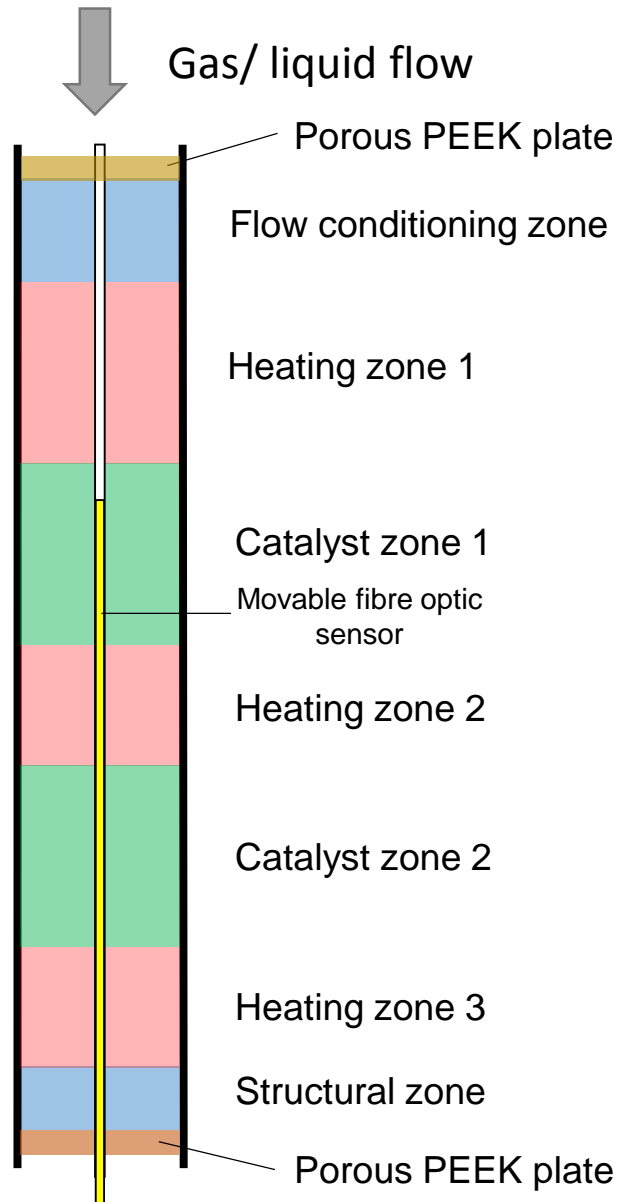
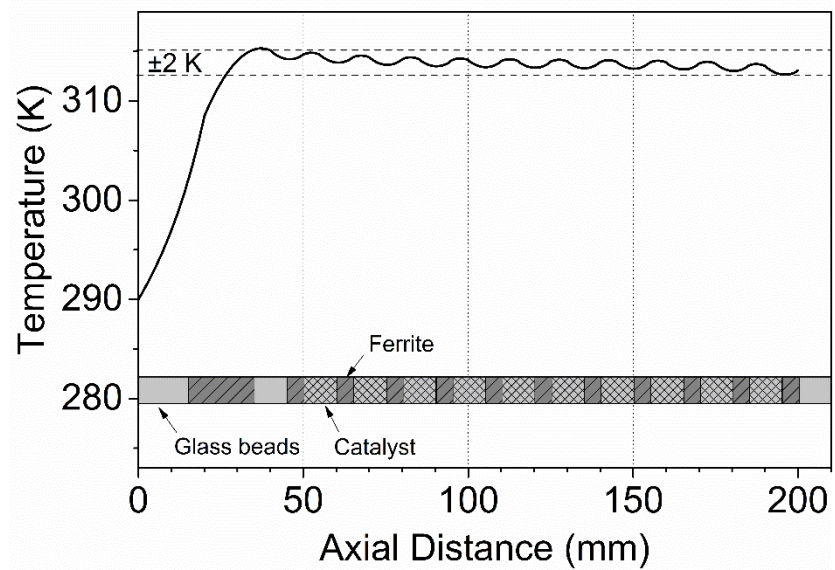


Figure 1

a)



b)

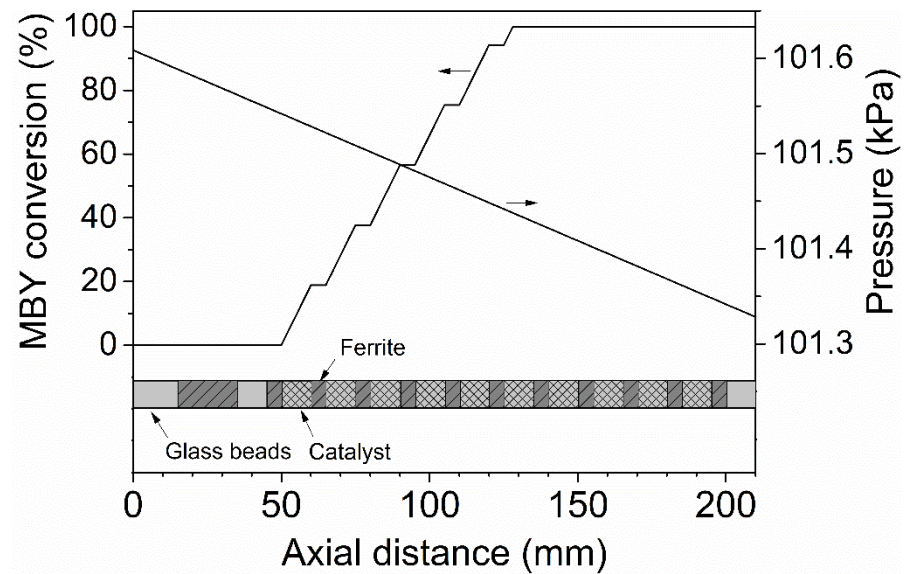


Figure 2

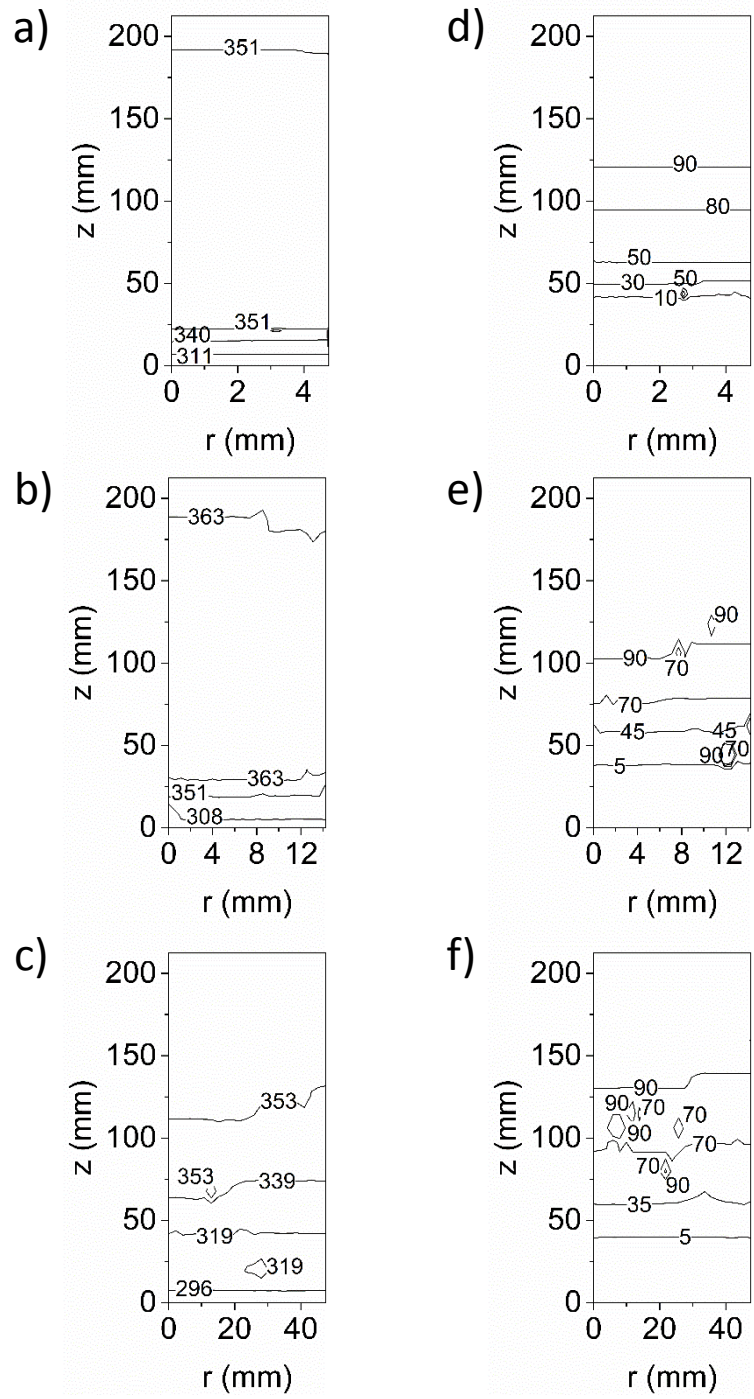


Figure 3

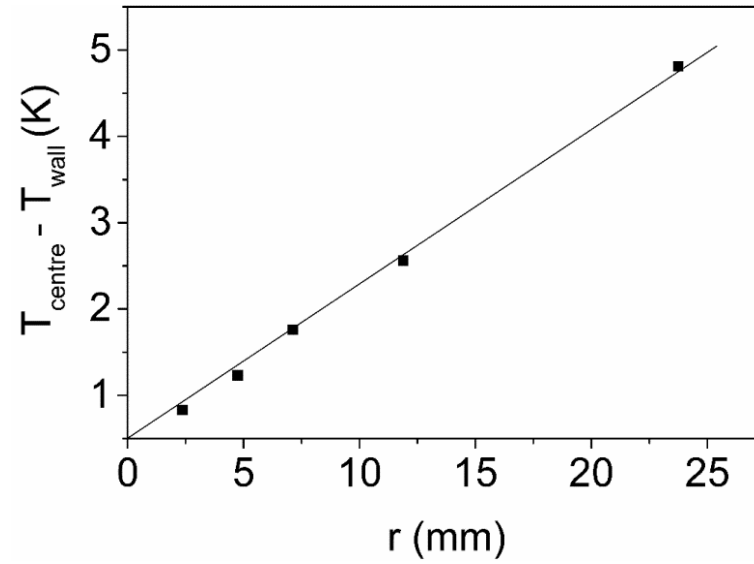


Figure 4

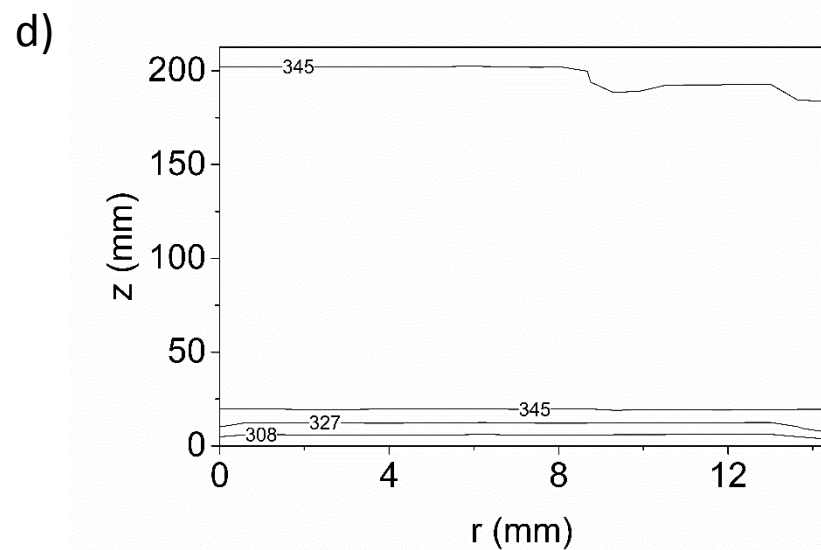
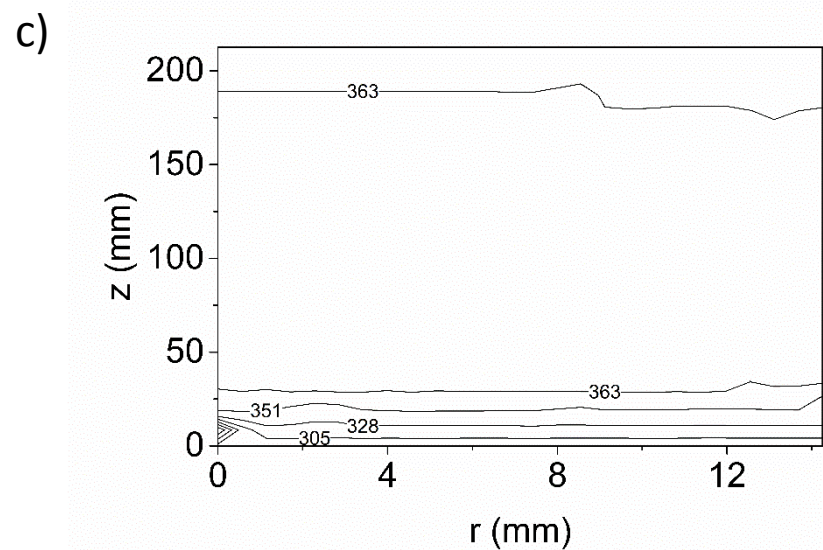
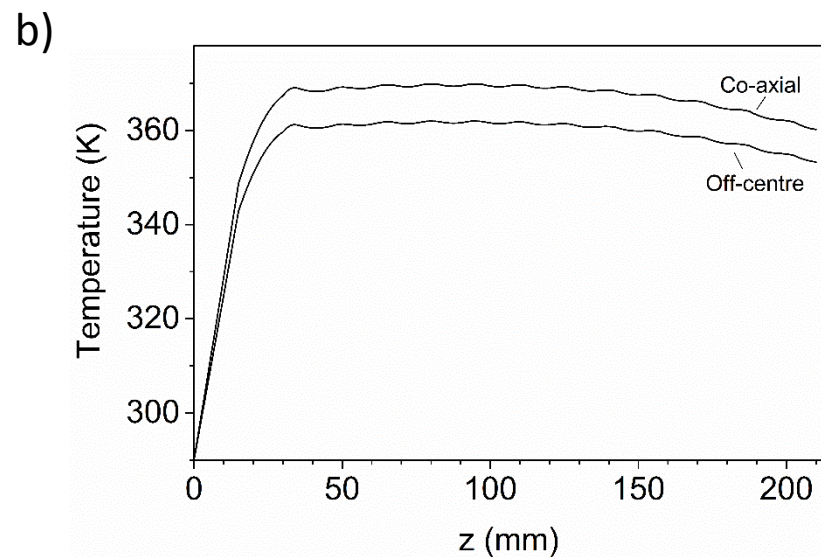
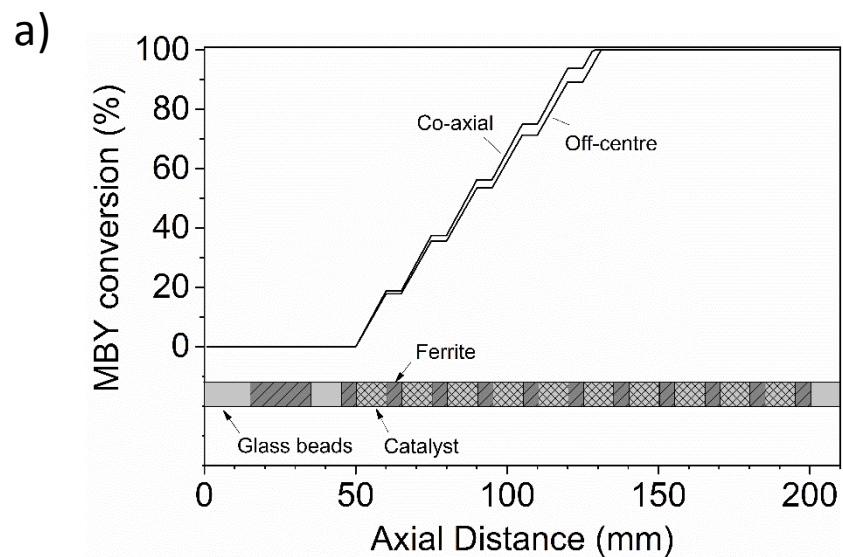


Figure 5

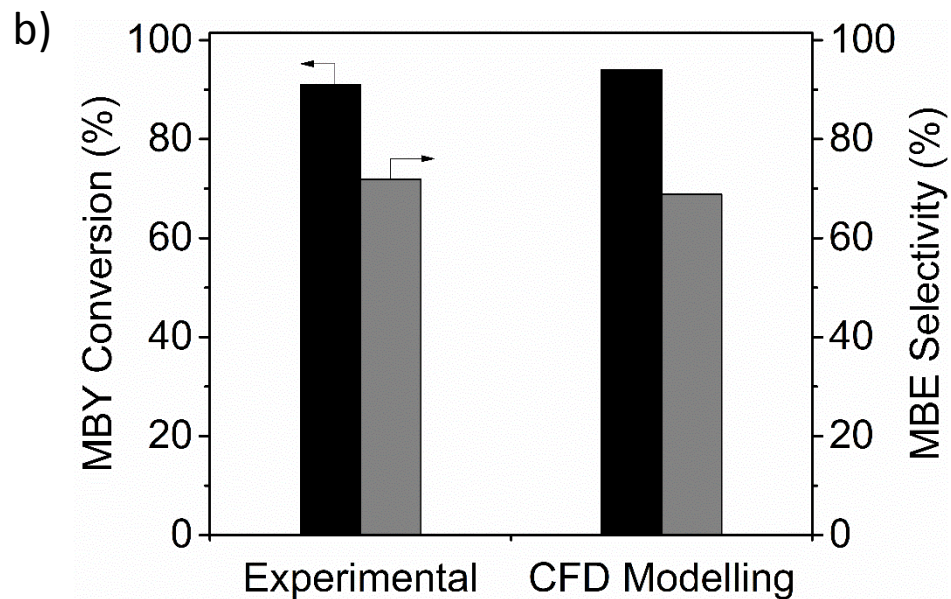
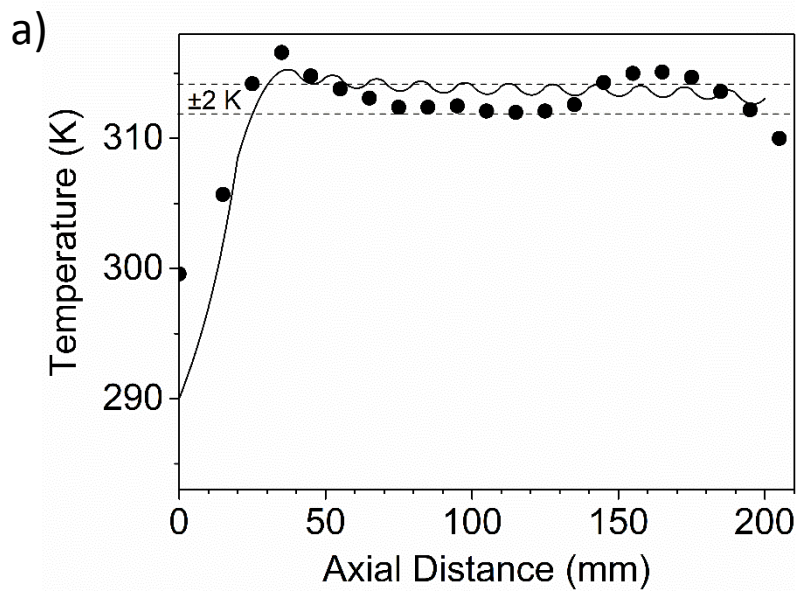


Figure 6

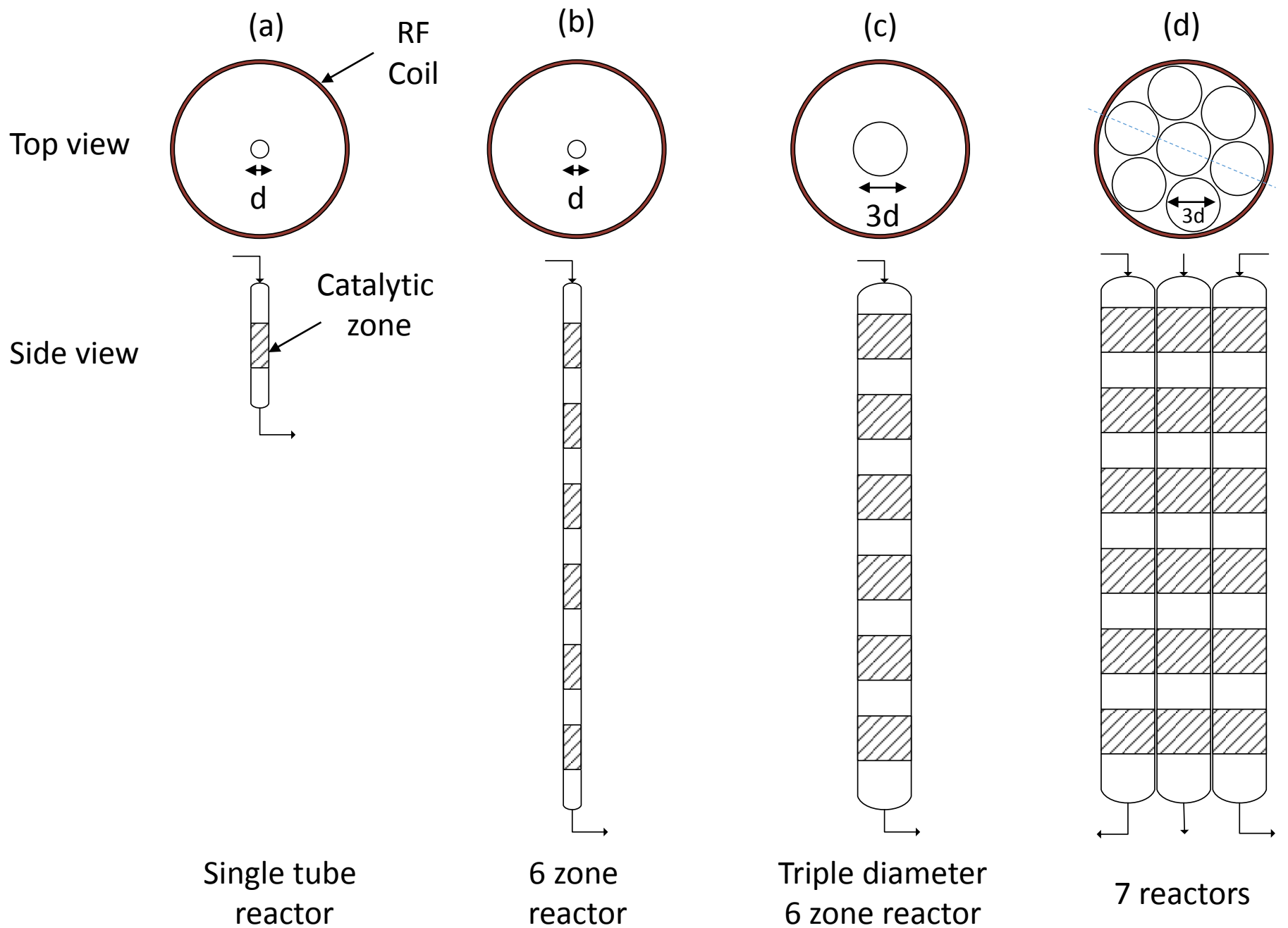
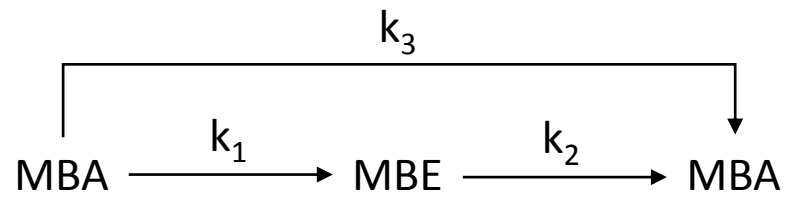


Figure 7



Scheme 1